Surface reflection of 3D scour models in Particle-Image-Velocimetry experiments

Ulrich Schuster[1,*], Daniel Quosdorf[1], Karl Ritter[2], Michael Manhart[1]

[1]Chair of Hydromechanis, Technische Universität München, München, Germany
[2]Munich School of Engineering, Technische Universität München, München, Germany
[*]corresponding author: ulrich.schuster@tum.de

Abstract This study investigates reflections at surfaces of construction materials in Particle-Image-Velocimetry measurements. The considered set-up is a half-page three dimensional model of a scour hole around a cylindrical bridge pier. The applied strategies are either absorbing or transmitting the incoming light energy by using fluorescent coating (Rhodamine B) and black-anodized aluminium, or acrylic glass. The intensity of surface reflections is dependent on its local curvature. Each method has its specific advantages and reduces surface reflections considerably. A fluorescent coating leads to thin reflective layers and very low background noise as a band-pass filter is required at the camera. Black-anodized aluminium is strongly absorbing incoming light; especially at a convex surface reflections disappear completely. Transmitting material (acrylic glass) reduces reflections tremendously. But as a side effect the whole specimen is illuminated, thus, the background noise is high in the area of the model surface.
Keywords: PIV, surface reflections, scour

1 Introduction

The particle-image-velocimetry (PIV) is a state-of-the art measurement technique to visualize and to quantify a flow field. It provides various possibilities from a two component (2C-2D) up to a time-resolved three component set-up (3C-4D). One of the main advantages consists in being able to gain flow field properties non-intrusively within an whole area of interest. A light-sheet provided by a laser illuminates a small non-isotropic volume (quasi 2D) in a flow. The thickness in the z-direction is one order of magnitude smaller than the ones in the x- and y-direction (see sketch in figure 1). Hence, it is considered as a 2D plane in which only the u- and v-components of a velocity field can be measured (Mono-PIV).

The distribution of the wall shear stress is of great importance in order to understand the scour process occurring around a cylindrical bridge pier [3]. Wall shear stress is evolving over time as the scour hole deepens and reaches asymptotically an equilibrium state (clear-water conditions) [2]. To investigate the flow field in a scour hole and associated processes it is important to freeze the geometry at a specific point in time. Predicting the wall shear stress correctly, it is crucial to minimize the distance to the wall of the first measurement point [8]. Therefore, we use a fixed geometry of a scour hole, i.e. milled in some construction material, and to be able

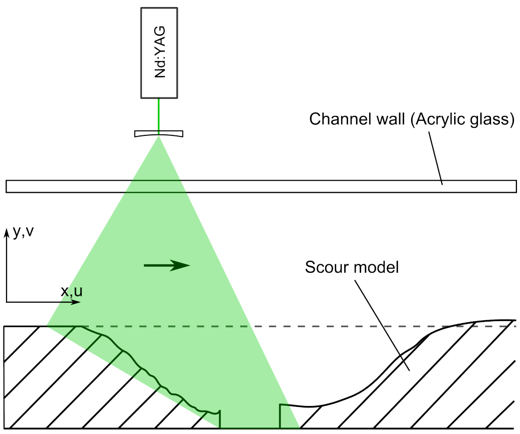

Fig. 1 Sketch of light sheet

measure the flow properties with PIV. To obtain quantities of the velocity distribution close to the wall surface reflections have to be avoided as far as possible.
A bright reflection layer at the wall impedes the calculation of displacement vectors in the area of interest; due to a lack of contrast no particles can be observed. Further, the specific case of a scour hole presents the challenge of a rough 3D-shaped surface with high diffusive reflective pattern. Therefore, the quality of PIV measurements can be decreased tremendously. Firstly, the overall light intensity is increased in the images that implies a poor contrast between particles and background (signal-to-noise-ratio). A second aspect is the obtainable distance from the first valid measurement point to the wall. The third issue is related to the sensor of the camera. Using a CCD-chip, strong reflections can lead to blooming effects in an image such as bright lines, and reduce the visible area strongly. In the worst case irreversible damages to the sensor (blind spots) occur. For these reasons we aim to find a material which can be used for building a model of scour around a bridge pier and suppresses any reflections to gain velocity distributions as close to the wall as possible.
Beside analytical methods to damp the impact of surface reflections [1], [9], there are three different constructional ways to minimize surface reflections according to [5]: absorbing the light energy, increasing the transmittance of the material, and directed specular reflections. However, specular reflection can not be used in a 3D-shaped model with complex curvature and limited optical accessibility. Consequently, we concentrate on absorbing the light energy or increasing the transmittance of a model material. The concept of absorbing energy consists of two strategies: fluorescent coating and black surface.
In section 2 the experimental set-up will be outlined followed by an description of the applied methods in section 3. The obtained results together with their discussion are presented in section 4. Finally, a summary and conclusion will be given in section 5.

2 Experimental set-up

The experiments were conducted in a miniature flume due to reasons of practicability and handling. The walls of the flume were made of acrylic glass to ensure optical accessibility. A laser (Nd:YAG) illuminated the experiment with 80% of the maximum available energy from above via a light arm. The combination of a concave cylindrical lens with a diverging lens at the exit of the light arm produced the light sheet. Perpendicular to the illumination a CCD-camera was mounted with an objective of 105mm focal length. The 12-bit-camera recorded grey values for the light intensity in the range of 0 (black) and $2^{12}-1=4095$ (white). The symmetric half-page models were placed at the wall next to the camera to keep the optical path as short as possible. Table 1 gives an overview of important parameters and figure 2 sketches the experimental set-up. A tank (1) provided water for the experiment, the cycle was started by a pump (2) and with a valve (3) the discharge could be roughly controlled in the system. After the inlet into the channel the flow calmed with the help of a pack of spherical glass marbles (4) with a diameter of 1.6cm. The flow straightener (5) ensured an uniform span wise velocity distribution before the test section (6) was reached. At this point, the models were installed and illuminated from above; the camera was mounted perpendicular from the side. An additional valve (7) purged the channel from air bubbles.

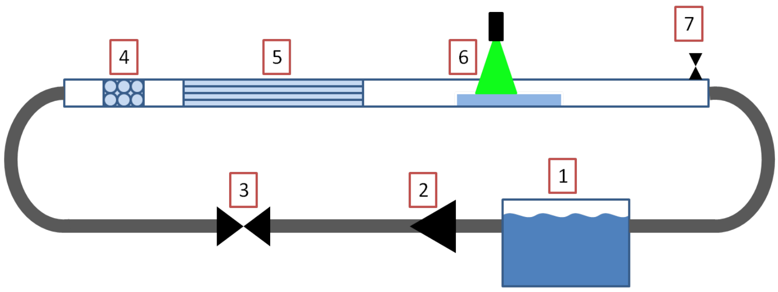

Fig. 2 Sketch of experimental set-up

Channel	Length	$100cm$
	Width	$20cm$
	Height	$6cm$
Model	Length	$12cm$
	Width	$6cm$
	Height	$2.5cm$
Illumination	Pulsed laser	Nd:YAG
	Wavelength	$532nm$
	Energy (max.)	$190mJ$
	Pulse duration	$8ns$
	Light sheet thickness	$2mm$
	Time delay	$1500\mu s$
Imaging	Camera	CCD
	Resolution	$2048 \times 2048px$
	Bit depth	$12bit$
	f-number	4
	Scaling	$28\mu m/px$
	Magnification	0.26
Fluid	Water, Density	$1000kg/m^3$

Table 1 Overview of experimental parameters

3 Methods

We conducted PIV experiments with small-scale scour models to investigate the reflective properties of different construction materials. As the models were of manageable size due to easy handling, it was not the main goal to be able to conclude any flow properties from these measurements. The geometry of a scour hole was based on laser-distance-sensor measurements of [6] conducted after one hour from the start under clear-water conditions. To freeze the geometry at this specific state we milled it in Poly-Vinyl-Chloride (PVC), acrylic glass and aluminium. The applied strategies were either absorbing or transmitting the energy of the laser light. Therefore, we compared a fluorescent coating on PVC combined with a band-pass filter at the camera (case A), black-anodized aluminium (case C) according to the study of [7], and acrylic glass (case B) with uncoated PVC as the reference case.

The strategies A and C can be described as a surface treatment. In the fluorescent case we coated a PVC model with transparent car finish in combination with Rhodamine B. This coating was applied with air brush technique repeatedly to ensure a preferably constant thickness of the fluorescent layer. The aluminium model was anodized after milling. During an anodization process an oxide layer grows on the surface of an aluminium specimen by applying electric current to the model submerged in an acid bath. This layer increased the electric resistance, thus, the voltage grew accordingly and broke the oxide layer at certain points: pores developed. These pores were filled with black colour, hence, the surface was coated with a highly light-absorptive layer.

Further, the models were symmetric and only one half was installed in the flume to avoid camera inclination and related errors. As the reflections of a surface are strongly dependent on its local curvature, we defined three different sections within the scour hole to evaluate the performance separately: concave (cc), convex (cx), and planar (pl).

We evaluated locally light intensity profiles for each curvature. I.e. along a certain column in an image, which represents a curvature area, the intensities were plotted and compared. As characteristic quantities we considered: the peak light intensity I_{peak} of the reflection in the wall region, the width of the reflection peak (measured in pixels δ_{px} and microns $\delta_{\mu m}$), the average intensity I_{avg} in the wall region, and the mean and standard deviation of the background light intensity μ_{noise} and σ_{noise}, respectively, calculated by the light intensities in the part of the image above the interface of the light sheet and the wall. As the width of the light intensity peak could not be determined distinctly, we defined it as follows:

$$\delta = I_{peak} \pm \sigma^* \tag{1}$$

with σ^* as the standard deviation of the peak intensity. In other words, the thickness of the reflective layer at the surface equals two times the standard deviation of the maximum intensity. To compute the standard deviation we assumed the intensity as Gaussian distributed, therefore σ^* corresponds to 60.5% of the peak. Furthermore, we introduced a second comparative measure that combines the average of light intensity in the reflective layer and the width of reflection at the wall. This value can be interpreted as an area of light intensity, thus, the smaller this value becomes the less surface reflections are observed.

$$\alpha = I_{avg} \cdot \delta_{px} \tag{2}$$

4 Results

Figure 3 shows the images from PIV measurements of each tested case. Sub-figure i) represents the reference case (untreated PVC). Picture ii) depicts the fluorescent Rhodamine B coated model, in iii) the acrylic glass is displayed and image iv) corresponds to the black-anodized aluminium model. Table 2 gives an overview of the obtained results. The three different strategies of surface treatment are compared, based on the aspects described in section 3, to the reference case depending on three characteristic curvatures: concave (cc), convex (cx), and planar (pl).
Figure 4 displays the light intensity profiles for each curvature. The profiles were extracted from the corresponding images along vertical lines (see green lines in figure 3) starting from top to bottom. Thus, the area within an image which corresponds to the cut face is also recorded in these plots. I.e. after the intensity profiles having reached the wall (from left to right with increasing pixel index) the plot represents reflected noise at the cut face of the half page symmetric specimens.

4.1 Reference case

The reference case shows that for a three dimensional geometry strong reflections appear all over the model. It can be noted that there are different areas of reflectivity, as planar parts do not glean as strong as curved sections; especially concave areas are indicated by high reflective behaviour. The observed light intensity exceeded in any case the upper threshold of the CCD-sensor (4095 counts), and the width of the reflection layer ranged from 12 up to 53 pixels, which corresponded to 336 and to 1484 μm in our set-up. Further, the rest of the image is enlightened by reflected light, i.e. the background noise is at a level of 269 counts.
As the untreated PVC surface is highly reflective, the intensity profiles increase the closer it comes to the wall. The curved areas (concave and convex) are characterized by a bright area of about 200 pixels width distinct to the wall. In general, untreated PVC would not lead to useful results in PIV as the reflections impede the evaluation of displacement vectors near the wall by introducing high noise. The introduced α-value ranges from $4.1 \cdot 10^4$ in the planar region up to $18.2 \cdot 10^4$ at the concave surface.

4.2 Case A: fluorescent coating (Rhodamine B)

Using a fluorescent coating on a PVC model, decreases the reflections strongly, but a dependency on the surface curvature can be obtained. Especially concave parts lead to a high peak intensity (>4095) at the wall and sprinkle the light, whereas in convex and planar shaped sections the fluorescent coating has a peak intensity of 1996 and 1425 counts, respectively. Thus, it reduces the brightness in the convex and planar parts by a factor of 2.05 and 2.87. Looking at the thickness of the reflective layer, the Rhodamine B did perform very well. The amplitude of the intensity peak was still large but the fluorescent coating reduced the width of the reflection to 10 pixels (280 μm) at the concave wall, and down to 2 pixels (56 μm) in the convex section. A general effect was obtained as the light intensity of the whole image was decreased, compared to all other applied methods. The necessity of having used a band-pass filter with fluorescent coating has resulted in a low background noise (12 counts in average, i.e. reduced by a factor of 22.42 compared to reference) in the remaining image, which comes clear in every profile plot. Distant parts from the wall (pixel no. 200–1000) within an image appeared to be darker than in the reference case and strategies B and C. The filter eliminated the major part of non-fluorescent reflections, e.g. when the light sheet entered the channel. This effect can be seen in all intensity profiles and is independent on the local curvature of the surface. The Rhodamine B coated model reveals a very sharp trend of intensity profiles. Directly at the wall there is a single peak of reflected light, and the remaining parts of the image have only little noise. The influence of the curvature of a model comes clear as the observed reflected light intensity at the wall decreases from the maximum recordable value (4095 counts) at the concave shape down to about the half (1996 counts) at a convex shaped wall to 1425 counts at a planar surface. The reflective layer ranges from 10 pixels at the concave surface to only 2 pixels at a convex shaped part of the model. At the planar surface the thickness is about 7 pixels. The fluorescent coating reduces the α-value to $3.39\cdot10^4$ for the concave shape, in the planar region to $0.65\cdot10^4$, and to $0.18\cdot10^4$ in convex area.

4.3 Case B: transmitting model (Acrylic Glass)

The transmitting model, made of acrylic glass, appeared to avoid reflections effectively, since the peak values ranged from 380 in the concave up to 1081 counts in the convex section. Thus, it reduced the peak intensity by a factor up to 11. The light passed the surface without reflecting considerably, hence, the whole specimen started to glow. Therefore, it appears brighter than the ones of absorbing coatings, i.e. the background noise in the images was higher than in case A or C. Out-of-focus parts of the three dimensional model became visible as the whole material was enlightened. Hence, the intensity profiles start to fluctuate increasingly the more material appears in the background (see concave and convex section). In the convex and planar areas we could define the thickness of the reflective layer to 5 pixels (140 μm) and to 13 pixels (364 μm), respectively. However, in the concave part this definition could not be applied which assumes a Gaussian shape of the light intensity distribution at the wall. As the acrylic glass specimen started to glow, we can roughly describe the light intensity as a step function; directly at the concave wall the intensity rose up to its local peak (380), remained shortly at a certain level, and continued to increase inside the model. Therefore, we could not evaluate all comparative quantities and indicated them with * in table 2. Furthermore, we can not determine without a doubt if the peaks of the intensity profiles due to the surface reflections are exactly at the boundary or slightly above or inside the model. Here, not only surface reflections come into account but also reflections at the bottom of the transparent model or body reflections inside the model, i.e. inclusions or fine cracks in the material reflect incoming light waves. Inspecting the α-value acrylic glass performs effectively: $0.43\cdot10^4$ and $0.59\cdot10^4$ for the convex and planar section, respectively. No value could be determined for the concave shape as no reflective width could be defined here (step function).

4.4 Case C: absorbing coating (Black-anodized aluminium)

The black-anodized aluminium model reduced surface reflections in all curvature areas. The concave part revealed a thin reflective layer (5 pixels or 140 μm) with a peak intensity of 2135 counts. Thus, the reduction coefficient of the peak intensity could be computed to 1.92 and the reflective layer thickness diminished by a factor of 10.6. The convex area had basically no surface reflections at all, as we observed the peak light intensity at 88 counts. Considering the mean background noise (82 counts) and its standard deviation (32 counts) it comes clear that the reflection of a convex wall can not be distinguished from common noise. For this shape the reduction coefficients concerning light intensity and reflection layer, could be determined to 46.53 and 9.67, respectively. The planar surface appeared to be effective as well. The maximum reflected light intensity could be determined to 1052 counts, which corresponds to a reduction coefficient of 3.89 and the layer thickness reached only 2 pixels (or 56 μm), i.e. it was 6 times thinner than the reference. The part of an image above the model is characterized by a certain background noise that is irrespective of the surface treatment. When the model material contributes to the background of the image (from pixel index 1000 to the wall) the light intensity decreases since the black surface absorbs scattered light. Directly at the wall, we observe clear but thin peaks in the intensity profiles. For the convex curvature we can not define the position of the wall by selecting a characteristic peak. Only the combination of all intensity profiles and looking at the PIV image enabled us to define a certain peak as the result of surface reflections. The α-value emphasizes the very good performance of this strategy as it ranges from $0.82\cdot10^4$ for the concave shape to $0.02\cdot10^4$ in the convex area.

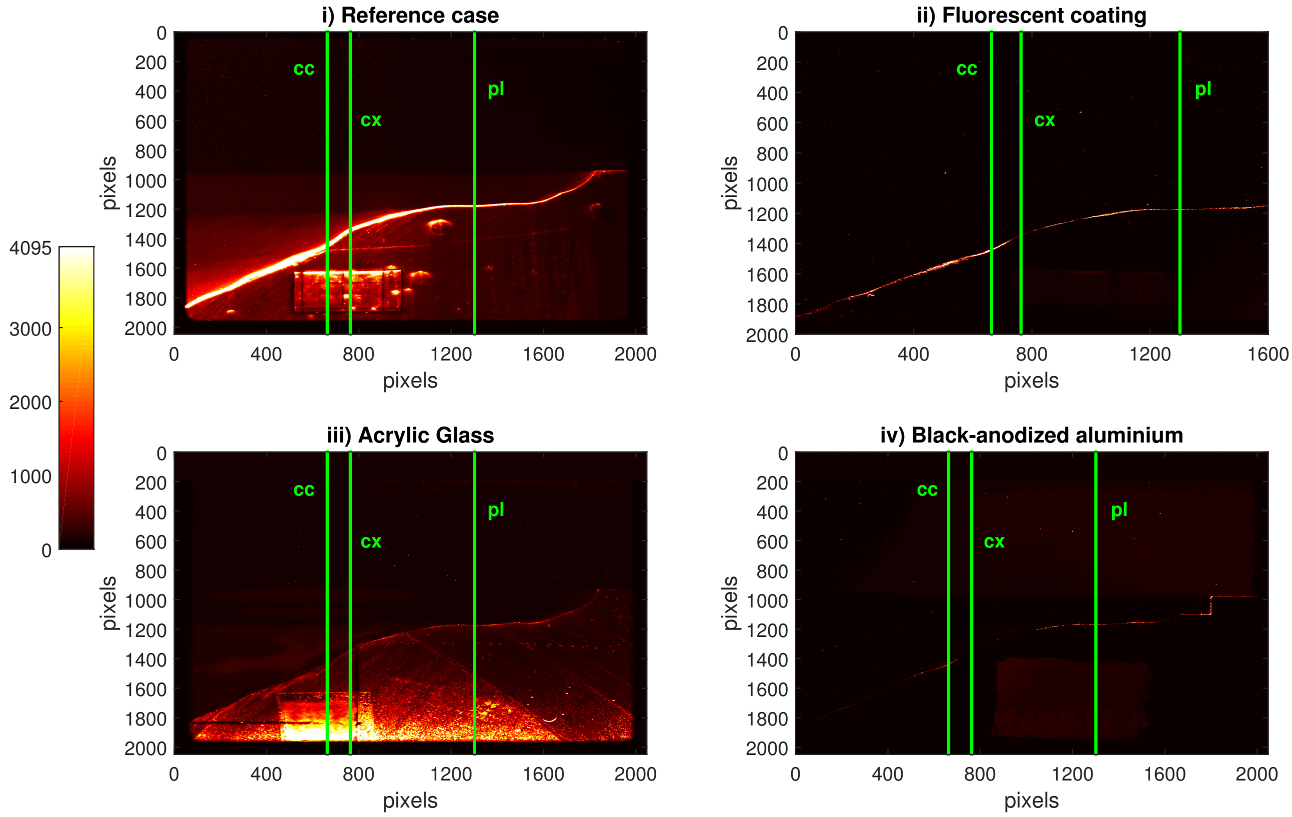

Fig. 3 PIV images of all applied strategies and the reference case, colour map ranges from 0 to 4095 counts

Case	Reference: PVC			A: Rh.B			B: Acryl.Glass			C: Black-anod. Alu.		
Curvature	cc	cx	pl	cc	cx	pl	cc	cx	pl	cc	cx	pl
I_{peak}	>4095	>4095	>4095	>4095	1996	1425	380	1081	635	2135	88	1052
I_{avg}	3432	3870	3404	3389	890	926	*	849	455	1635	74	459
$\rho_I = \frac{I_{ref}}{I_i}$ { peak	1	1	1	1	2.05	2.87	10.77	3.79	6.45	1.92	46.53	3.89
avg	1	1	1	1.01	4.35	3.68	*	4.56	7.48	2.10	52.29	7.42
δ_{px}	53	29	12	10	2	7	*	5	13	5	(3)	2
$\delta_{\mu m}$	1484	812	336	280	56	196		140	364	140	(84)	56
$\rho_\delta = \frac{\delta_{ref}}{\delta_i}$	1	1	1	5.30	14.50	1.71	*	5.80	0.92	10.60	(9.67)	6.00
$\mu_{noise} \| \sigma_{noise}$	269 | 177			12 | 8			125 | 38			82 | 32		
$\rho_{noise} = \frac{\mu_{noise,ref}}{\mu_i}$	1			22.42			2.15			3.28		
$\alpha = I_{avg} \cdot \delta_{px} [\cdot 10^4]$	18.2	11.2	4.1	3.39	0.18	0.65	*	0.43	0.59	0.82	(0.02)	0.09

Table 2 Overview of the observed reflection quantities in each case

5 Summary & Conclusions

In this study, we evaluated the reflective behaviour of a three dimensional scour model by applying three different strategies, such as fluorescent coating (Rhodamine B), transparent material (acrylic glass), and absorbing surface (black-anodized aluminium). All these methods have led to tremendous improvements of the quality of PIV images in comparison to the reference case. Using a fluorescent coating is effective in planar of convex shapes. The reflective layer at concave curvatures diminishes but the maximum light intensity reaches still high levels. A considerable advantage consists in a very low background noise as an installed band-pass filter eliminates light of a certain wave length corresponding to the one of the incoming laser light. The implementation of such a coating brings some difficulties. First, an appropriate varnish has to be found which binds the fluorescent

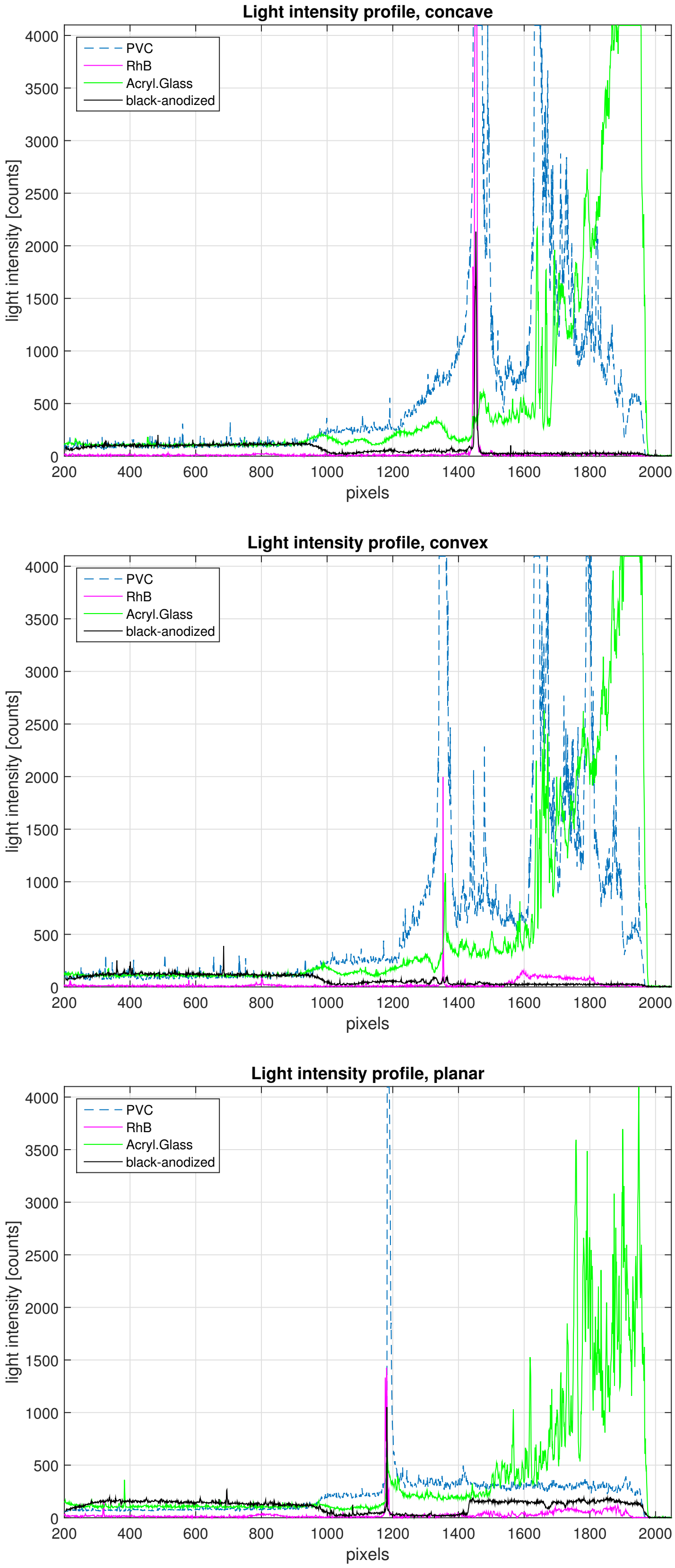

Fig. 4 Intensity profiles of concave (top), convex (middle), planar (bottom) wall

particles. Secondly, the three dimensional shape of the geometry requires to paint the surface in thin layers by air brush. Hence, this procedure has to be repeated several times to ensure a sufficient thickness of the coating. Further, any dust particles should be avoided in order to keep the varnish clean. Such particles would act as additional reflective sources and decrease the performance of the fluorescent coating. In general, the impact of temperature has to be considered using fluorescent coatings. Especially Rhodamine B is highly sensitive to temperature [4], i.e. the quantum efficiency of such a dye strongly decreases with increasing fluid temperature (quenching effect).

The acrylic glass model reduces surface reflections strongly for any curvature. Low light intensities and reflections at the surface would allow to correlate displacement vectors close to the wall even at complex geometries. The reflective layer is either very thin as it has low influence on the quality of the PIV images or it may even be located inside the model that the wall appears with high contrast (step function). Incoming light illuminates the transparent material, thus, the background light intensity of the image is higher than the one of absorbing materials. Therefore, body reflections and ageing of the material (fine cracks) come into account as well.

Black-anodized aluminium reduces surface reflections strongly. The width of the reflection and its peak intensity are important aspects to assess the performance of a surface treatment strategy. Inspecting both aspects separately, and their combination (α-value) it comes clear that black anodized aluminium is the most effective strategy to suppress surface reflections. Further, no band-pass filter at the camera is needed, no issues occur to choose the right painting strategy (e.g. dust), the performance of the material is comparatively insensitive to temperature, and no problems arise due to material ageing.

Further investigations could be done with full 3D models. In such a set-up the cameras must be inclined to access the scour hole completely. Therefore, we would recommend to conduct Stereo-PIV measurements. First, the whole impact of the three dimensional shape geometry would make an appearance. Secondly, one could additionally gain flow properties from such an experiment.

Acknowledgements This study was supported by the Deutsche Forschungsgemeinschaft (DFG) under the grant no. *Ma2062/11-1*.

References

[1] KÄHLER, C. J., SCHARNOWSKI, S., AND CIERPKA, C. On the uncertainty of digital PIV and PTV near walls. *Experiments in Fluids 52*, 6 (May 2012), 1641–1656.

[2] MELVILLE, B. W., AND COLEMAN, S. E. *Bridge Scour*. Water Resources Publications, LLC, Highlands Ranch, USA, 2000.

[3] MUTLU SUMER, B., AND FREDSOE, J. *The Mechanics of Scour in the Marine Environment*. World Scientific, Singapore, 2002.

[4] NATRAJAN, V. K., AND CHRISTENSEN, K. T. Development of fluorescent thermometry methods for microfluidic systems. In *14th Int Symp on Applications of Laser Techniques to Fluid Mechanics* (Lisbon, 2008).

[5] PATERNA, E., MOONEN, P., DORER, V., AND CARMELIET, J. Mitigation of surface reflection in PIV measurements. *Measurement Science and Technology 24*, 5 (Apr 2013).

[6] PFLEGER, F. *Experimentelle Untersuchung der Auskolkung um einen zylindrischen Brückenpfeiler*. PhD thesis, Technische Universität München, 2011.

[7] ROSTAMY, N., SUMNER, D., BERGSTROM, D., AND BUGG, J. Local flow field of a surface-mounted finite circular cylinder. *Journal of Fluids and Structures 34* (Oct 2012), 105–122.

[8] SCHANDERL, W., AND MANHART, M. Reliability of wall shear stress eestimation in front of a wall mounted cylinder. In *10th Workshop Direct and Large-Eddy Simulation* (Limassol, 2015).

[9] SCIACCHITANO, A., AND SCARANO, F. Elimination of PIV light reflections via a temporal high pass filter. *Measurement Science and Technology 25*, 8 (Jul 2014).